International Journal of High Speed Electronics and Systems
Vol. 25, Nos. 1 & 2 (2016) 1640009 (13 pages)

DOI: 10.1142/S0129156416400097

World Scientific
www.worldscientific.com

Photo-Electrochemical Etching in the Process of Direct H2 Generation by Illumination of GaN-Based Material Structures Immersed in Water

A. Usikov

Nitride Crystals Inc., 181 E Industry Court, Suite B, Deer Park, NY 11729, USA
alexander.usikov@nitride-crystals.com

S. Luryi

Sensor CAT at Stony Brook University, Stony Brook, NY 11794-3717, USA
serge.luryi@stonybrook.edu

A. Nikiforov

Boston University, Photonics Center, 8 St. Mary's St., Boston, MA 02215, USA
alnik@bu.edu

H. Helava

Nitride Crystals Inc., 181 E Industry Court, Suite B, Deer Park, NY 11729, USA
heikki.helava@nitride-crystals.com

Yu. Makarov

Nitride Crystals Inc., 181 E Industry Court, Suite B, Deer Park, NY 11729, USA
yuri.makarov@nitride-crystals.com

M. Gouzman

Sensor CAT at Stony Brook University, Stony Brook, NY 11794-3717, USA
michael.gouzman@stonybrook.edu

Received 4 May 2016
Accepted 29 October 2016

Hydrogen is considered a promising candidate for energy storage. We investigated the cleanest way for hydrogen production by direct photo electrolysis of water with GaN/AlGaN based p-n structures used as working electrodes. Besides the H_2 production rate, an important consideration is the material etching (corrosion) that accompanies the photo-electrochemical process. The GaN-based structures were grown on sapphire substrates by the chloride hydride vapor phase epitaxy and used as a photo anode immersed into an aqueous electrolyte. For a p-n GaN/AlGaN structure we observed a H_2 production rate of 0.6 mL/cm^2×h. Corrosion of the electrode proceeds in two steps. First, there is a near vertical etching process, which is associated with defects in the material and penetrates deep into the structure. Subsequently, the process involves etching of n-type layers in lateral direction resulting in the formation of voids and cavities. The lateral etching is due to net positive charges arising from the spontaneous and piezoelectric polarization in the structure and positively charged ionized donors in the space charge region of the p-n junction.

Keywords: HVPE; III-N structures; photo-assisted electrochemical process

1. Introduction

Hydrogen gas is a promising energy carrier. Energy generation by oxidation of hydrogen is harmless to the environment as it leaves only water as a by-product. The source of hydrogen production is also water, which is abundant on Earth. It is important to produce hydrogen cleanly. A number of technologies for hydrogen generation have been proposed that use solar energy directly or indirectly. These include, among others, the thermo-chemical water decomposition process driven by a concentrated solar system, the generation of hydrogen through biomass or through photosynthetic microorganisms, and hydrogen production by electrolysis of water [1]. To ensure a clean cycle of use, the electrolysis itself can be driven by renewable electricity. For example, one can decompose water electrochemically using photovoltaic solar cells connected directly to electrolyzer electrodes. Particularly attractive is direct splitting of water in photo cells with direct semiconductor/liquid contacts. This is a simple technology that avoids significant costs involved with the use of a separate electrolyzer wired to p-n junction solar cells. Another attractive advantage of the direct photo electrolysis of water at a semiconductor surface is the ease with which an electric field can be created in a semiconductor p-n structure and at a semiconductor/liquid junction.

In the direct water splitting process, an immersed semiconductor material catalyzes the decomposition of water into H_2 and O_2 gases by solar irradiation of its surface. The energy required to split water molecules is generated by the absorption of sunlight in the semiconductor. The solar water splitting process may be spontaneous under illumination if the electrochemical redox potentials of the oxygen evolution reaction (OER) and the hydrogen evolution reaction (HER) in an electrolyte are exceeded by the energy gap of the semiconductor. The wide-gap semiconductors, such as GaN and many InGaN alloys meet this requirement [2-5].

An exemplary diagram of the photo-electrochemical water splitting using an n-GaN layer and an alkaline electrolyte is given in Figure 1. The absorption of solar photons in the semiconductor generates excited electron–hole pairs that are split by the semiconductor band-bending at the n-GaN electrode/electrolyte interface (Mott-Schottky junction [6]). The upward band-bending is due to the establishment of equilibrium between the n-GaN Fermi level and the redox potential of the electrolyte solution. The band bending moves the excited holes (h^+) toward the interface and the excited electrons (e^-) into the interior of the semiconductor. The external circuit brings (e^-) to the cathode, where they take part in HER ($4H_20+4e^- \rightarrow 2H_2+4OH^-$) that yields ions of OH^- (anions) and molecules of H_2. The anions complete the circuit at the GaN-anode by pairing with (h^+) that leave the semiconductor in OER ($4OH^-+4h^+ \rightarrow O_2+H_2O$), yielding molecules O_2 and H_2O. The HER occurs on platinum cathode and OER occurs on the n-GaN photo anode. Figure 2 illustrates the process.

Not all of the electron-hole pairs excited by illumination in the semiconductor immersed in an electrolyte do participate in OER and HER. The extent of the space-charge region in n-GaN layers (arising from the upward bend bending of the order of 1 eV near the surface [7, 8]) is typically too thin (tens of nm) in comparison with the light

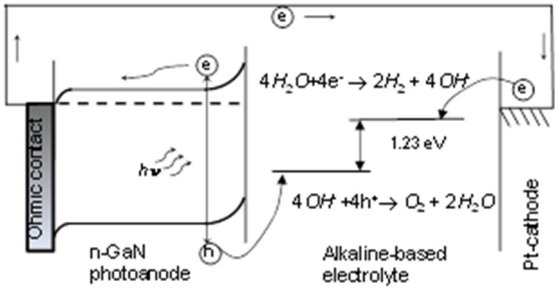

Fig. 1. A generic diagram of the photo electrochemical water splitting using n-GaN as a working electrode (photo anode).

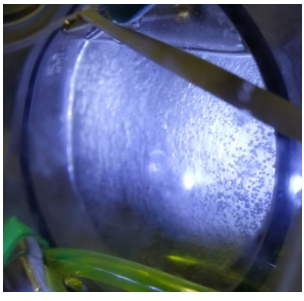

Fig. 2. Image of a GaN-based 2-inch structure immersed into KOH-based electrolyte and fully covered by small gas bubbles.

absorption depth (300-500 nm). The gas generation rate is further reduced by carrier recombination at the surface and in the bulk of the semiconductor layer.

Another process having a negative effect on the gas evolution reaction is photo-corrosion or etching of the electrode material [6]. The corrosion is an issue when the photo electrode is n-type, because the upward band-bending at the interface promotes the transfer of photo-generated holes to the electrolyte. The holes at the semiconductor/ electrolyte interface have much higher energy (more than 1 eV) relative to the reduction potential for (O2/H2O) redox couple (OER) in the electrolyte and oxidize not only water but the photo electrode itself.

In contrast, the downward band-bending in p-type materials transfers to the electrolyte the photo-generated electrons with little excess energy. The resultant HER process leaves the surface of the photo-electrode almost intact chemically [5, 7, 8]. However, there have been relatively few studies of the p-type III-N materials as photo electrodes in the photo-electrochemical process.

The direct water photo electrolysis features a relatively low photocurrent density (on the order of tens mA/cm^2, because of the weakly concentrated sunlight used to illuminate the photo electrodes. The typical values of the concentration factor range from 1× to 20×. Higher values of the concentration factor require a solar tracking system, resulting in electrolyte heating, and necessitating an efficient heat sink. This does not sit well with the concept of a simple design and low cost expected from a photo electrolysis system.

In this work we use as working electrodes GaN/AlGaN p-n structures with p-type GaN layer on the surface to investigate both the H_2 production rate and the material corrosion inherent in the photo-electrochemical process. The structures were grown on a sapphire substrate by chloride hydride vapor phase epitaxy (HVPE).

2. Samples and Experimental Techniques

Several 4-10 μm-thick GaN layers and AlGaN/GaN p-n structures were grown by chloride HVPE on c-plane 2-inch sapphire substrates in a conventional horizontal-flow reactor. The growth procedure included in-situ sapphire substrate treatment followed by

multilayer structure growth consisting of a composite AlN/ $Al_xGa_{1-x}N$ (x ~ 0.6) buffer layer and 4 pairs of $Al_xGa_{1-x}N$ (x ~ 0.1-0.15)/ $Al_xGa_{1-x}N$ (x~0.03-0.08) stress control layers (SCL) on a sapphire substrate. The p-n structure was grown on the top of the SCL in the same run. The basic AlGaN/GaN structure included a 50-100 nm-thick GaN active region co-doped by Zn and Si to have emission at 420 nm [9], which was sandwiched between p- and n- $Al_xGa_{1-x}N$ barriers (x ~ 0.05–0.12), all grown on a 2-3 μm thick n-GaN:Si contact layer (n ~ 2-4 × 10^{18} cm^{-3}). A 0.5-1 μm-thick p-type GaN contact layer doped with Mg covers the structure. The Mg doping produces a hole concentration up to 10^{18} cm^{-3} in the contact layer. GaN layers were grown without SCL. Details of the structure growth and characterization can be found elsewhere [10]. Note that it was the p-type GaN layer surface that served as a photo-electrode (working electrode) in this work.

In the first set of experiments, we studied the photo-electrolysis specific etching for the AlGaN/GaN p-n structures. The 2-inch wafers were immersed in a potassium hydroxide water electrolyte (5.7 weight % of KOH, pH=14) under external bias of +2.5 V and under solar irradiation. As a counter electrode a 2-inch diameter Ni plate was positioned parallel to the working electrode at a distance of about 3 cm. The working electrode was irradiated by a 150 W Xe lamp (AM 1.5 standard spectrum) with a concentration factor of 20×. The irradiated area (spot size) was adjusted to 1.3 inch (33 mm) diameter. The electrical contact to the sample (working electrode) was made through a metallic clamp with In pads. The structures were partly immersed in the electrolyte. A segment of the structure, which was used to hang the whole wafer by the clamp, was above the electrolyte to avoid a short circuit. The whole process of photo electrolysis took about 6 minutes.

The second set of experiments was focused on the production of H_2 and O_2 gases by the photo electrolysis using the KOH aqua electrolyte. Fig. 3 shows photographs of the setup manufactured for these experiments. A 2-inch GaN-based p-n structure was used as a working electrode. An area of 1.3-inch diameter was in contact with the KOH electrolyte. A Ni plate that used a counter electrode had a hole to irradiate the working electrode by the Xe lamp. The H_2 gas was produced on Ni electrode, the O_2 gas was produced on GaN electrode. The gases were collected by graduated cylinders.

After the experiments, the samples were cleaved and their surface morphology and luminescence properties were examined in both top-view and cross-sectional configurations by high-resolution scanning electron microscopy (SEM) and cathodoluminescence (CL) spectroscopy and monochromatic CL imaging, respectively. The CL measurements were performed on a Gatan MonoCL2 system. The CL spectra from three distinct areas of the samples described above were acquired by rastering a 10 kV electron beam over an area of 20 μm × 15 μm. For CL spectra from cross-sections, an 8 nA beam current was used. For CL spectra from the top surface, a slightly smaller beam current of 4 nA was used to mitigate electron beam induced charging on the top surface.

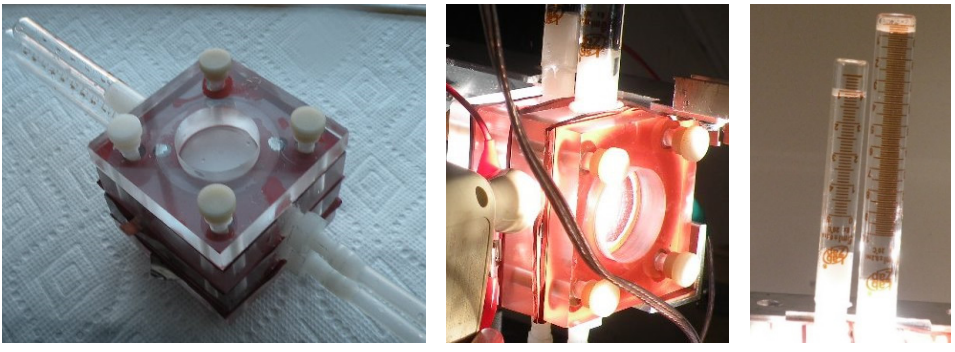

(a) (b) (c)

Fig. 3. Photographs of the experimental setup. (a) general view, (b) under operation, (c) separate graduated jars (gas tube collectors) to collect O_2 and H_2 gases.

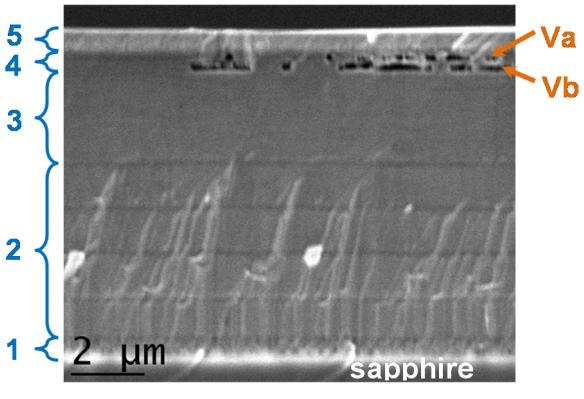

Fig. 3. Cross-sectional SEM image of the AlGaN/GaN p-n structure after photo electrolysis. (a) Area 2. No peculiarities related to the photo-electrochemical etching are observed. Va and Vb denotes voids formed in the the GaN active layer and the n-AlGaN barrier layer, respectively. (1) AlN/AlGaN buffer, ~0.65 µm; (2) AlGaN/AlGaN four pairs, 4.97 µm; (3) n-GaN:Si contact layer, ~2.5 µm; (4) n-AlGaN barrier layer, ~0.5 µm and GaN:(Zn+Si) active layer, ~0.2 µm; (6) p-GaN contact and p-AlGaN barrier layers, ~0.66 µm.

3. Results

After the experiment, three areas could be identified on the structure surface by the naked eye: Area 1 that was not immersed into KOH, Area 2 that was immersed into KOH but not illuminated by the Xe lamp, and Area 3 that was immersed into KOH and illuminated by Xe lamp. Area 3 on the surface of the structure appears to be dimmer than its surroundings.

Fig. 3a shows SEM images of cross sectional views of the same sample taken at Area 3 on the surface. All layers of the structure can be distinguished. The structure total thickness is about 9.5 µm. Note that in the experiment a +2.5V bias was applied to the p-type top layer of the structure from an external power source, i.e. the structure was a photo anode. During the experiment, the measured value of the photocurrent was found

to decrease from 4.3 mA to 2.2 mA (0.5-0.25 mA/cm^2). Total thickness of the p-type layers is about 0.7 μm. Two rows of micro-voids in Fig. 3 can be ascribed to the photo-electrochemical etching. The position of the voids in the stack of layers in the structure suggests that these voids are formed in the GaN active layer (the voids denoted as Va) and in the underlying n-AlGaN barrier layer (the voids denoted as Vb). The micro-voids can spread laterally and overlap leading to the formation of a large-size cavity. Note that such peculiarities were not observed in a cross-sectional view of Area 2 (the area that was immersed into the electrolyte but not illuminated by the Xe lamp).

Fig. 4 shows the large-size cavity that formed after the photo-electrolysis process was performed on another AlGaN/GaN p-n structure but having higher photocurrent of 5.6-9.7 mA (0.65-1.1 mA/cm^2) under the same illumination. The large-size cavity may result in delamination of the p-layers from the structure. Fig. 5 shows a scanning micrograph of surface morphology in Area 3 of the sample in Fig. 3. Pits and large open cavities on the surface are attributed to the photo- electrochemical process. The pits density is about 7×10^8cm^{-2} and it varies over the sample surface up to $(1\text{-}2)\times10^9$ cm^{-2} in the most defective areas near the microcracks. The CL spectra acquired from the sample surface have a weak emission at about 360 nm and a dominant broad peak centered around 420 nm as shown in Fig. 6a. The strongest luminescence was measured from the area illuminated by the Xe lamp (Area 3) where the density of nonradiative defects was likely to decrease as a result of the photo-electrochemical etching. The coarser surface morphology in Area 3 may also improve the light extraction efficiency.

The dominant emission can be ascribed to the active layer located at a depth of 0.5-0.6 microns from the surface. Although the 10 kV beam penetration is limited to about 0.4 microns in depth [11], the electron beam spreading and various surface irregularities,

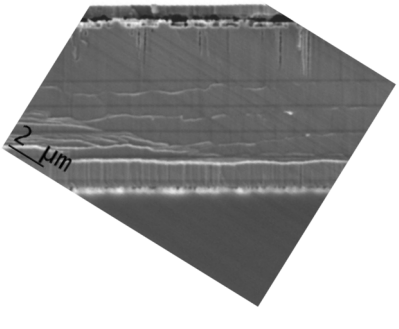

Fig. 4. Cross-sectional SEM image of Area 3 of another AlGaN/GaN p-n structure. Overlapped micro-voids that formed under higher photocurrent than in the Fig. 2sample off the p-layers from the structure created a large-size cavity that may delaminate or peel the layer.

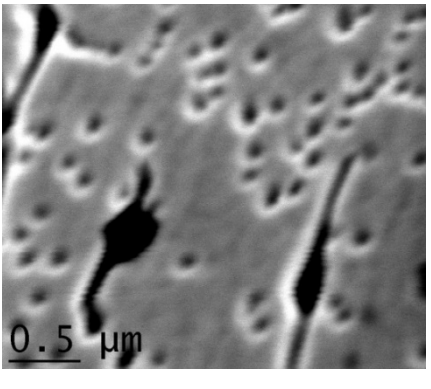

Fig. 5. SEM image of surface morphology after photo-electrochenical etching of AlGaN/GaN p-n structure in Fig. 3. Pits density is about 7.7×10^8 cm^{-2}.

such as pits and micro-cracks, allow beam electrons to reach active region located underneath the p-type contact layers and creates electron-hole pairs within the active layer. Their subsequent recombination results in an enhanced CL signal observed from the structure surface. A 1-3 µm thick Mg-doped p-type GaN layer grown in a separate run had a PL peak emission near 440 nm. Broad CL spectra overlap the emission from the p-GaN contact layer in Fig. 6.

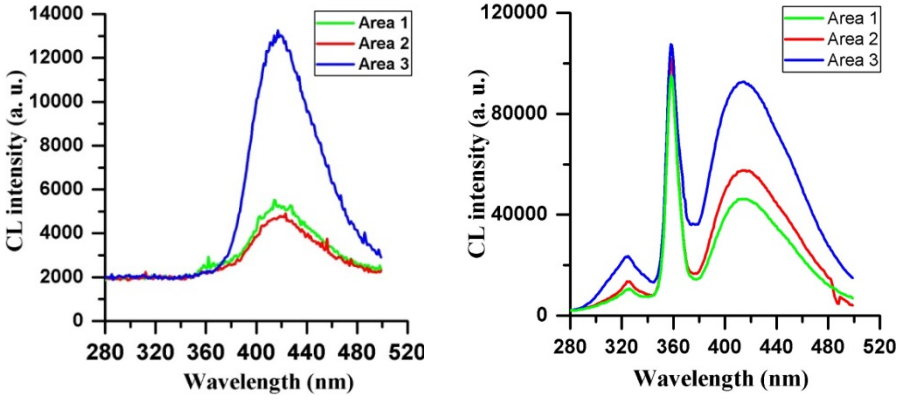

Fig. 6. CL spectra taken from the AlGaN/GaN structure in Fig. 3 from the surface (a) and from cross section of the sample (b). Emission from the active region at ~420 nm is observed in both configurations.

To further elucidate the origin of the luminescence peaks, the CL spectra were acquired from cross-sections from the three distinct areas defined above. The spectra are shown in Figure 6b. A strong broad emission from the active region at 414-420 nm is accompanied by a strong signal from the n-GaN contact layer at around 360 nm. Emission in the range of 324 to 331 nm could be ascribed to the AlGaN barriers. The rastered area included the substrate for reference purposes, for example, for a proper identification of the substrate-SCL layer interface in the monochromatic CL mapping.

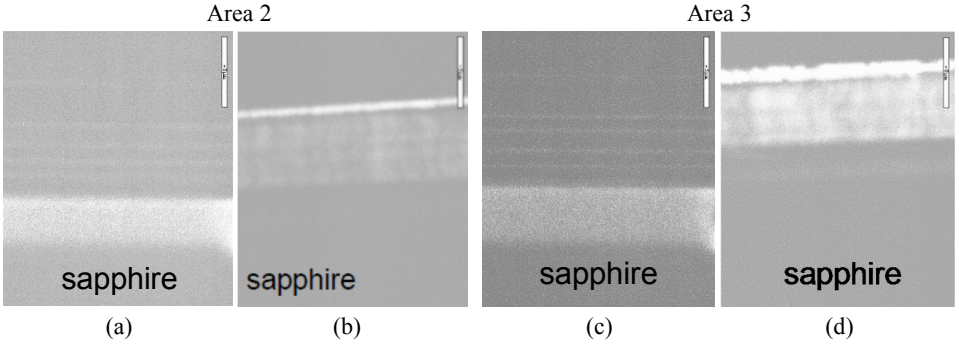

Fig. 7. Cross-sectional monochromatic CL maps after photo-electrochemical etching acquired at (a) 324-331 nm; and (c) 420- nm for sample in Fig. 1. The scale bar is 5 µm.

The cross-sectional monochromatic CL maps acquired at the corresponding wavelengths of 324-331 nm and 420 nm for both samples are shown in Figure 7. The maps at 324-331 nm and at 360 nm for both samples are very similar as they indicate that the corresponding luminescence emissions are coming from the AlGaN layers and from the GaN barriers in the bulk of the structure, respectively. The 420 nm emission corresponds to the GaN active region and is mainly localized within about a micron thick region near the top surface and correlates with subsurface void formation and top layer delamination in the area etched and illuminated by the Xe lamp (Area 3).

4. Discussion

It is clear that the photo electrochemical etching follows paths of the photo-current flow. The current flow paths in III-N GaN/AlGaN or GaN/InGaN materials, especially at low current, are non-uniform and can be associated with the shunt conductance in an extended defect system of grain boundaries, threading dislocations, local regions with irregular alloy composition enriched by metallic atoms (Ga or In), and others extended defects [12].

Voids observed in the SEM images in Figs. 3-4 suggest that the process of their formation goes in two stages. During the first stage, the etching process starts via channels (or shunts) in the extended defect system of the structure penetrating the p-type layers all the way into the underlying n-type layers. The shunts could be threading defects, grain boundaries and micro-cracks attributed to the mosaic structure of the as-grown structures. During the second stage, the etching on the n-type AlGaN barrier and GaN active layer proceeds in a lateral direction resulting in the formation of voids and cavities underneath the p-type layers. Although the p-type layers of the structure remained unetched, the top surface exhibited a lot of pits.

The UV portion of the illumination light gets effectively absorbed in the p-GaN contact layer (at a depth of about 0.2-0.3 um from the surface) leading to the formation of excited electron–hole pairs. These pairs can be separated further by either the internal electric field of the space-charge region in the p-n junction of the structure when they drift towards it or by the specific band-bending at the p-GaN layer/electrolyte interface. The potential barrier at the p-n junction is higher than the bend-bending at the surface of the p-GaN layer and the separation of the excited electron–hole pairs could be further affected by p-n junction resulting in the generation of a photocurrent. The photo-generated carriers may participate in two competitive processes in the structure employed as an anode and immersed into an electrolyte under irradiation: (1) oxygen evolution reaction (OER) and (2) photo-etching of GaN and GaN-based materials. However, because of the too thick p-GaN layer (0.5-0.6 μm thick) the excited electron–hole pairs recombine mostly at the structure surface and in the p-layer before being separated by the p-n junction producing as a result a relatively low photocurrent. It appears that relatively low photocurrent flows non-uniformly through the structure selecting paths with higher conductivity, such as threading defects and micro cracks.

We speculate that photo-generated holes could assist in oxidative decomposition of p-GaN, primarily in the vicinity of the threading defects forming dangling bonds of Al^{3+} and Ga^{3+} ions. Hydroxide ions (OH-) from the electrolyte would then attack the Al^{3+} and Ga^{3+} dangling bonds and form hydroxides $Al(OH)_3$ and $Ga(OH)_3$ [13, 14]. Dissolution of the hydroxides would lead to the formation of soluble Al_2O_3 and Ga_2O_3. Continuous formation and dissolution of the oxides in the solution would further simulate the etching process.

The etching process may move deeper into the layers via the threading defects. The Mg-doped p-type GaN and AlGaN layers have ionized Mg- acceptors and may screen partly the positive charge of the dangling bonds preventing the etching of the p-type layers but still allowing the etching to proceed along the threading defects. Indeed we did not observe any appreciable etching of the top p-layers. However, some micro-cracks and numerous pits associated with etching were observed on the top surface as can be seen in Figure 5. It is likely that these pits are associated with dislocations.

The step involving lateral etching in Figs. 3-4 can be explained considering effects resulting in a positive charge at layer interfaces. It is know that spontaneous and piezo-electric polarization between AlGaN/GaN layers in the structure results in a formation of a net positive charge at their interface [15]. Figure 8 shows a net positive charge at the AlGaN/GaN interface in the AlGaN layer caused by the sum of the net spontaneous polarization and piezoelectric polarization between the AlGaN and GaN layers in the structure growing along the c-direction [15].

The positive +Qπ charge at the bottom side of the thick GaN layer in Fig 8a has a negligibly small effect on the charges at the AlGaN/GaN interface due to a presence of large number of electrons, traps and defects between the interface and the bottom portion of the thick underlying GaN layer. The sheet charge due to polarization in the AlGaN layer surface and at the interface is balanced also. To keep neutrality, the positive charge at the interface is compensated by electron accumulation forming a two dimensional electron gas (2DEG) close to the interface [15], the source of electrons in the 2DEG is the surface states [16] (Ibbetson et al., 2000).

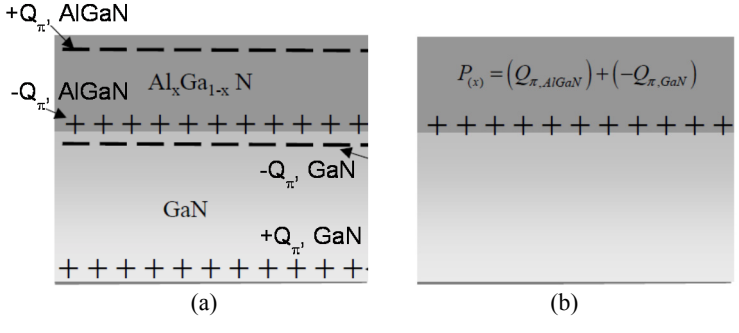

Fig. 8. CL Polarization charges in an AlGaN/GaN structure. (a) Charge polarization in individual layers of the structure (b) a net positive charge at the AlGaN/GaN interface in the AlGaN layer [15].

The structures in this work had a stack of doped GaN and AlGaN layers at the top (i.e the n-GaN active layer was sandwiched between n- and p-AlGaN barrier layers) that influences the net positive charge compare to that depicted in Fig. 8. First of all, negatively charged ionized acceptors (Mg-) in the p-AlGaN layer may screen positive polarization charge at the p-AlGaN barrier layer/n-GaN active layer interface. In addition, a thin n-GaN active layer is not fully relaxed and may have additional positive piezoelectric polarization charge at the n-GaN active layer/n-AlGaN barrier layer interface.

Then, n-AlGaN barrier also has a positive piezoelectric polarization charge at the interface with n-GaN contact layer beneath (see Fig. 1a for reference to the structure design). Note also that all thin AlGaN layers having higher composition in the AlGaN/AlGaN four-pairs structure, beneath the n-GaN contact layer, have a net positive polarization charge. However these layers are located deep in the structure, further away from the structure surface. Only two thin n-GaN active and n-AlGaN barrier layers are near the p-type layers and have positive piezoelectric polarization charge. An additional positive charge at the layer interfaces can be connected with positively charged ionized donors, which are Si+ presumably, in a space charge region of the p (AlGaN)-n (GaN) junction. This positive charge is located in the n-GaN active region too.

The net positive charge at the GaN/AlGaN n-n and p-n interfaces promotes OH^- ions from the electrolyte to form $Ga(OH)_3$ and (or) $Al(OH)_3$ hydroxides and the nitrogen vacancy sites and continue the etching process along the positive charge position forming lateral voids and large-size cavities.

When the etching process via threading defects reaches a layer with positive net charge it changes the etching direction from vertical to lateral presumably because of a stronger charge at the layer interface than that in the channel associated with threading defects and dangling bonds. When large threading defects, for example, large cracks are encountered the etching process may penetrate deeper into the structure as shown in Fig. 3b. However, the n-type AlGaN layer located at a depth from the surface switches the etching process from a vertical to a lateral direction due to a larger positive piezoelectric polarization charge at the layer interfaces.

Recent investigations of degradation mechanisms for similar HVPE-grown AlGaN/GaN p-n LED structures using multifractal analysis indeed demonstrated the existence of conductive paths (shunts) localized at threading defects (dislocations) [12]. In our AlGaN/GaN structures, the shunts are leakage paths for photo-currier flow that are responsible for non-uniform current spreading, diminishing the gas evolution reaction, and decreasing the efficiency of direct water photoelectrolysis. Low-defect GaN-based working photo electrodes are important for the photo electrolysis process by focusing on gas generation but not etching.

Separate experiments on photo electrolysis with an external power source using structures having GaN layers only demonstrated porous-like etching of a 5-6 μm thick n-GaN layer through the layer to the substrate. In p-n GaN structures having a p-GaN layer on the top the etching process was terminated on the p-n junction. Figure 9 shows SEM

images of the cross-sectional of two samples consisted of a n-GaN layer only and p-n GaN structure after the photo electrochemical etching in a KOH-based electrolyte. Both structures were grown using a thin AlGAn –based buffer later that was nor revealed in the SEM images in Fig. 6. The structures were anodes in the experiment. It seems the space charge region of the p-n junction associated with ionized acceptors and donors can prevent the etching spreading. We speculate that negative ions (OH^-), which participate in the etching reaction of GaN-based materials in the electrolyte, are screened by negatively charged ionized acceptors (Mg^-). At the same time, the positive charged ionized donors (Si^+) have negligible smaller effect in the reaction with the ions OH^-.

The H_2 production rate of 0.6 ml/cm^2×h in was measured for an optimized p-n GaN/AlGaN structure immersed in 8-11% KOH electrolyte under the Xe-lamp illumination only (concentration factor – ×15). The setup in Fig. 3 was used for the experiments. A 2-inch wafer was used as a working electrode. Gases that were generated on Ni-electrode and the GaN sample were collected in two separate graduated jars. After 30-40 minutes of operation, there was 2 to 2.4 times more gas collected in the jar above the Ni-plate than in the jar above the GaN sample. It proves that H_2 was generated on the Ni plate.

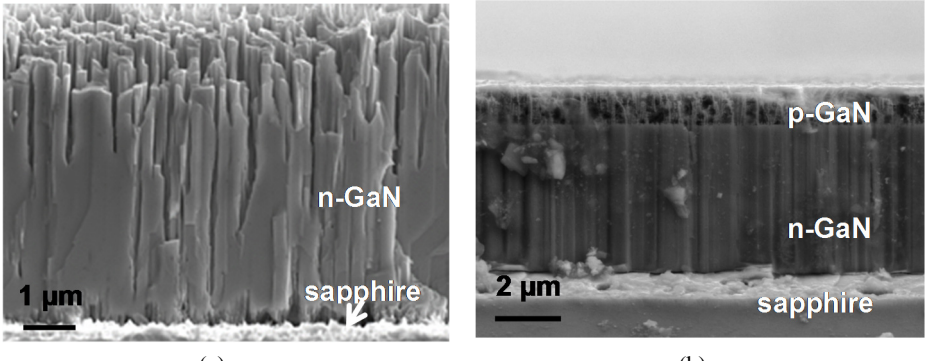

(a) (b)

Fig. 9. Scanning micrographs of cross-section of two GaN structures after the photo electrochemical etching. (a) a 7.8 µm thick n-GaN layer with porous-like etching pattern through the whole layer (b). a 5.9 un thick p-n GaN layers. The etching process was terminated at the p-n junction.

5. Conclusions

Two stages of photo electrochemical etching under conditions of light illumination and external power source were observed in a GaN/AlGaN p-n structure having p-type layers on the top. During the first stage, the etching process occurs near vertically via channels associated with defects in the structure and penetrates deep into the structure to n-type layers passing p-type layers. The p-type layers of the structure remain un-etched in the process. During the second stage, the process involves etching of the n-type AlGaN barrier and GaN active layer in a lateral direction resulting in the formation of voids and cavities beneath the p-type layers. The lateral etching is likely due to net positive charges

at the AlGaN/GaN interfaces arising because of spontaneous and piezoelectric polarization in the structure and positively charged ionized donors in the space charge region of the p-n junction. The H_2 production rate of 0.6 ml/cm^2×h was measured for a p-n GaN/AlGaN structure.

References

1. Turner, J., G. Sverdrup, M. K. Mann, P.-C. Maness, B. Kroposki, M. Ghirardi, R. J. Evans, and D. Blake. Renewable hydrogen production. International Journal of Energy Research, 32, 379-407 (2008). DOI: 10.1002/er.1372.
2. Waki, I., D. Cohen, R. Lal, U. Mishra, S. P. DenBaars, and S. Nakamura. Direct water photoelectrolysis with patterned n-GaN. Applied Physics Letters, 91(9): 093519 (2007).. http://dx.doi.org/10.1063/1.2769393.
3. Ohkawa, K., W. Ohara, D. Uchida, and M. Deura. Highly Stable GaN Photocatalyst for Producing H2 Gas from Water. Japanese Journal of Applied Physics, 52: 08JH04 (2013). http://dx.doi.org/10.7567/JJAP.52.08JH04.
4. Chen, S., and Wang L-W. Thermodynamic Oxidation and Reduction Potentials of Photocatalytic Semiconductors in Aqueous Solution. Chemistry of Materials, 24 (18): 3659–3666 (2012). DOI: 10.1021/cm302533s.
5. Aryal, K., B. N. Pantha, J. Li, J. Y. Lin, and H. X. Jiang. Hydrogen generation by solar water splitting using p-InGaN photoelectrochemical cells. Applied Physics Letters, 96: 052110-1 - 052110-3. (2010). DOI: 10.1063/1.3304786.
6. Wolff, N., M. Rapp, and T. Rotter. Electrochemical etching and CV-profiling of GaN. Physica Status Solidi (c), 2 (3): 990–993 (2005). DOI: 10.1002/pssc.200460607.
7. Rajeshwar, K., Hydrogen Generation from Irradiated Semiconductor-Liquid Interfaces. In: Solar Hydrogen Generation: Toward a Renewable Energy Future. K. Rajeshwar, R. McConnell, and S. Licht, (Eds.), Springer New York, 2008, pp 167-228: ISBN: 978038772809-4 (Print) 978038772810-0 (Online).
8. Liu, S.Y., Sheu J.K., Lee M.L., Lin Y.C., Tu S.J., Huang F.W., Lai W.C.. Immersed finger-type indium tin oxide ohmic contacts on p-GaN photoelectrodes for photoelectrochemical hydrogen generation. Optics Express, 20 (S2):A190 (2012). DOI: 10.1364/OE.20.00A190.
9. Usikov, A.S., D.V. Tsvetkov, M.A. Mastro, A.I. Pechnikov, V.A. Soukhoveev, Y.V. Shapovalova, O.V. Kovalenkov, V.A. Dmitriev, B. O'Meara, S.A. Gurevich, E.M. Arakcheeva, A.L. Zakhgeim, H. Helava. Indium-free violet LEDs grown by HVPE. Physica Status Solidi (c), 0 (7): 2265-2269 (2003). DOI: 10.1002/pssc.200303521.
10. Kurin, S., A. Antipov, I. Barash, A. Roenkov, A. Usikov, H. Helava, V. Ratnikov, N. Shmidt, A. Sakharov, S. Tarasov, E. Menkovich, I. Lamkin, B. Papchenko, and Yu. Makarov. Characterization of HVPE-grown UV LED heterostructures. Physica Status Solidi (c), 11 (3-4): 813-816 (2014). DOI: 10.1002/pssc.201300459.
11. Yacobi, B. G., and D. B. Holt. Cathodoluminescence scanning electron microscopy of semiconductors. Journal of Applied Physics, 59 (4): R1-R24 (1986). http://dx.doi.org/10.1063/1.336491.
12. Shmidt, N., E. Shabunina, A. Usikov, A. Chernyakov, S. Kurin, H. Helava and Yuri Makarov. Peculiarities of defect generation under injection current in LEDs based on A3N nano-structure. Physica Status Solidi (c), 12 (8): 1136-1139 (2015). DOI 10.1002/pssc.201400218.
13. Zhuang, D., Edgar, J. H. Wet etching of GaN, AlN, and SiC: a review. Materials Science and Engineering R Reports, R48: 1-46. (2005). DOI: 10.1016/j.mser.2004.11.002.

14. Macht, L., J.J. Kelly, J.L. Weyher, A. Grzegorczyk, P.K. Larsen. An electrochemical study of photoetching of heteroepitaxial GaN: kinetics and morphology. Journal of Crystal Growth, 273 (3-4): 347-356 (2005). DOI:10.1016/j.jcrysgro.2004.09.029.
15. Mishra U.K., P. Parikh, Y.F. Wu.. AlGaN/GaN HEMTs: An overview of device operation and applications. Proceedings of the IEEE, 90 (6): 1022-1031 (2002). DOI: 10.1109/JPROC.2002.1021567.
16. Ibbetson, J.P., P.T.Fini, K.D. Ness, S.P.DenBaars, J.S.Speck, and U.K.Mishra. Polarization effects, surface states, and the source of electrons in AlGaN/GaN heterostructure field effect transistors. Applied Physics Letters, 77 (2): 250-252 (2000). http://dx.doi.org/10.1063/1.126940.